

# Effect of pressure on the lattice properties in $\text{Eu}_{0.58}\text{Sr}_{0.42}\text{MnO}_3$ perovskite

S. Kaji<sup>a</sup>, G. Oomi<sup>a,\*</sup>, T. Eto<sup>a</sup>, E.V. Sampathkumaran<sup>b</sup>, A. Sundaresan<sup>c</sup>

<sup>a</sup> Department of Physics, Kyushu University, Ropponmatsu, Fukuoka 810-8560, Japan

<sup>b</sup> Tata Institute of Fundamental Research, Homi Bhabha Road, Mumbai-5, India

<sup>c</sup> Chemistry and Physics of Materials Unit, JNCASR, Jakkur P.O., Bangalore 560064, India

Available online 13 June 2005

## Abstract

The thermal expansion and lattice constants of  $\text{Eu}_{0.58}\text{Sr}_{0.42}\text{MnO}_3$  perovskite have been measured at high pressure. It is found that an anomalous expansion due to metal–insulator transition appeared on heating in the temperature dependence of the thermal expansion and its magnitude decreases with increasing pressure. The metal–insulator transition temperature,  $T_{\text{M-I}}$ , increases with increasing pressure. The lattice constants,  $a$ ,  $b$ , and  $c$  are found to decrease with increasing pressure but there is a large anisotropy in the lattice compression. The linear compressibilities are extracted to be  $1.5$ ,  $1.9$  and  $0.8 \times 10^{-3} \text{ GPa}^{-1}$  for  $a$ ,  $b$  and  $c$ -axis, respectively.

© 2005 Elsevier B.V. All rights reserved.

PACS: 77.84.Bw; 74.62.Fj; 65.40.De

Keywords: Manganese oxide; High pressure; Thermal expansion; Phase transition; X-ray diffraction

## 1. Introduction

Rare earth manganese perovskites  $\text{R}_{1-x}\text{A}_x\text{MnO}_3$  (R: rare earth element, A: Ca, Sr and Ba) have been investigated extensively because they show a wide variety of physical properties such as colossal magnetoresistance (CMR), metal–insulator (M–I) transition and so forth [1]. In these materials, the conduction electrons and localized spins are strongly coupled with lattice properties. It is worthwhile to investigate the response of the lattice properties to the external forces, such as pressure and magnetic field, to get a deep insight into the electronic and magnetic structure of these manganites.

$\text{Eu}_{1-x}\text{Sr}_x\text{MnO}_3$  ( $0 \leq x \leq 0.5$ ) are insulators due to a narrow  $e_g$  band width at ambient pressure but they show magnetic-field-induced M–I transition around  $x = 0.4$  [2]. For  $\text{Eu}_{0.58}\text{Sr}_{0.42}\text{MnO}_3$  ( $x = 0.42$ ), it has been revealed that it is a paramagnetic insulator (PMI) above 120 K, a canted antiferromagnetic insulator (CAFMI) down to 50 K, a spin glass insulator (SGI) below 45 K at ambient pressure in zero

field, and a ferromagnetic metal (FMM) under magnetic field [2]. M–I transition has been studied at high pressure and the metallic phase is found to stabilize under high pressure [3].

In the present work, we attempted to measure the thermal expansion, magnetostriction and lattice constants under high pressure in order to make clear the interplay between the lattice properties and electronic and magnetic properties. The results will be discussed using Grüneisen parameters and crystal structure transition.

## 2. Experimental procedure

Polycrystalline sample of  $\text{Eu}_{0.58}\text{Sr}_{0.42}\text{MnO}_3$  was prepared by calcining a stoichiometric mixture of  $\text{Eu}_2\text{O}_3$ ,  $\text{SrCO}_3$ , and  $\text{Mn}_2\text{O}_3$  at 1473 °C and sintering at 1673 °C [2]. Powder X-ray diffraction patterns showed the existence of single phase of orthorhombic structure. High pressure was generated by means of piston-cylinder device. The thermal expansion and magnetostriction were measured by using strain gauge method. The details of high pressure systems have been reported previously [4]. The lattice constants were measured by using X-ray diffraction at high pressures [5].

\* Corresponding author.

E-mail address: oomi@rc.kyushu-u.ac.jp (G. Oomi).

### 3. Results

#### 3.1. X-ray diffraction at high pressure

Fig. 1 shows the relative change of lattice constants,  $a$ ,  $b$  and  $c$  of  $\text{Eu}_{0.58}\text{Sr}_{0.42}\text{MnO}_3$  as a function of pressure. Because of the weak intensity of diffraction lines, there is a scattering in the data. We approximated these data as straight lines up to 14 GPa. Within experimental errors, there was no phase transition at room temperature up to 14 GPa. The linear compressibilities along each crystal axis are estimated by calculating the gradients of the straight lines in Fig. 1 to be,  $1.5$ ,  $1.9$  and  $0.8 \times 10^{-3} \text{GPa}^{-1}$ , respectively. This result indicates that the  $c$ -axis is harder than other axes. The volume was calculated using the formula,  $V = abc$ . In order to extract the bulk modulus  $B$ , observed data were fit to the Murnaghan–Birch equation. We obtained the value as  $B = 213 \text{ GPa}$  at room temperature, which is larger than those of other oxides, such as YBCO ( $\sim 160 \text{ GPa}$ ) [6] and LSCO ( $\sim 145 \text{ GPa}$ ) [7].

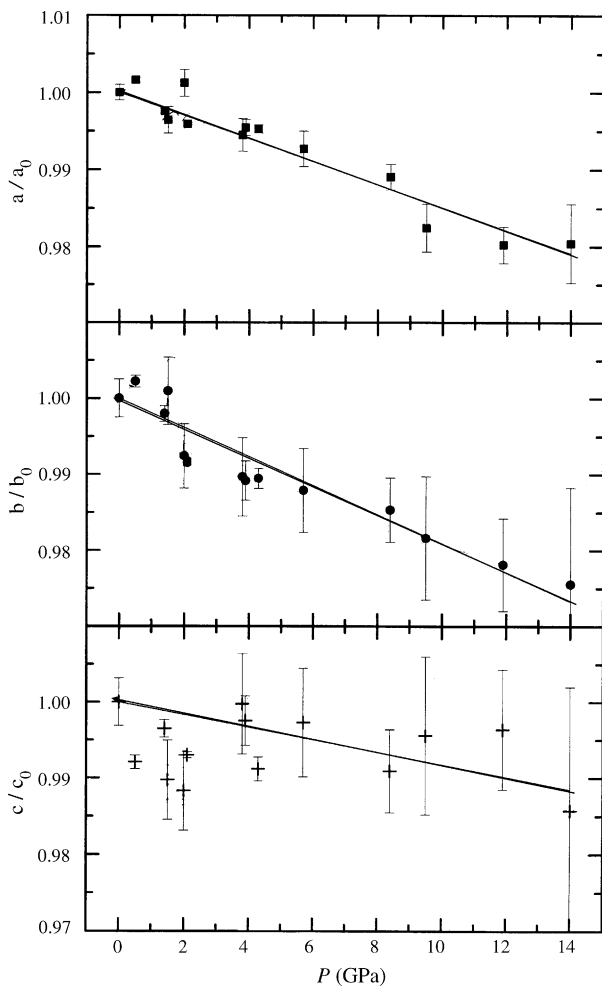


Fig. 1. The lattice constants of orthorhombic  $\text{Eu}_{0.58}\text{Sr}_{0.42}\text{MnO}_3$  at room temperature as a function of pressure.

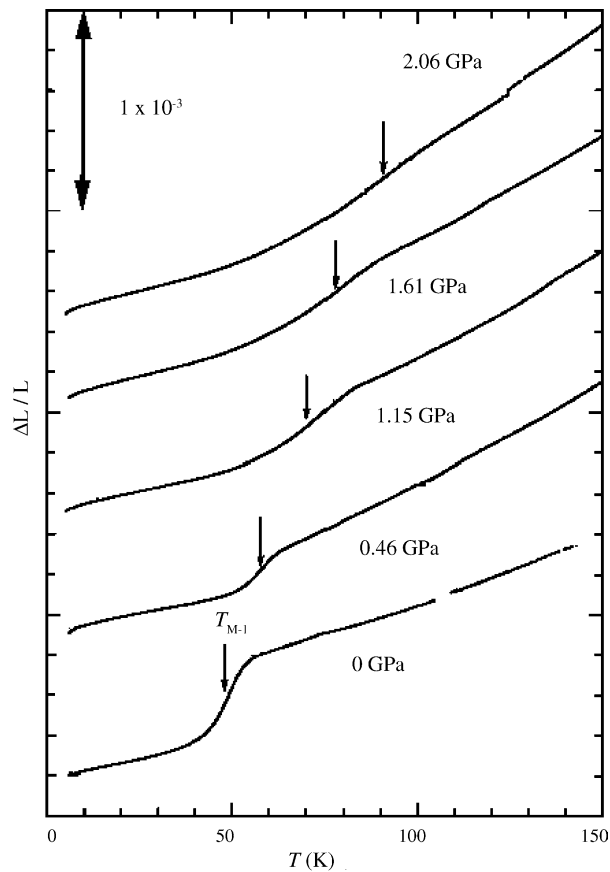


Fig. 2. Thermal expansion of ferromagnetic metal (FMM) phase on heating at high pressure. The arrows show the metal–insulator transition temperature  $T_{M-I}$ .

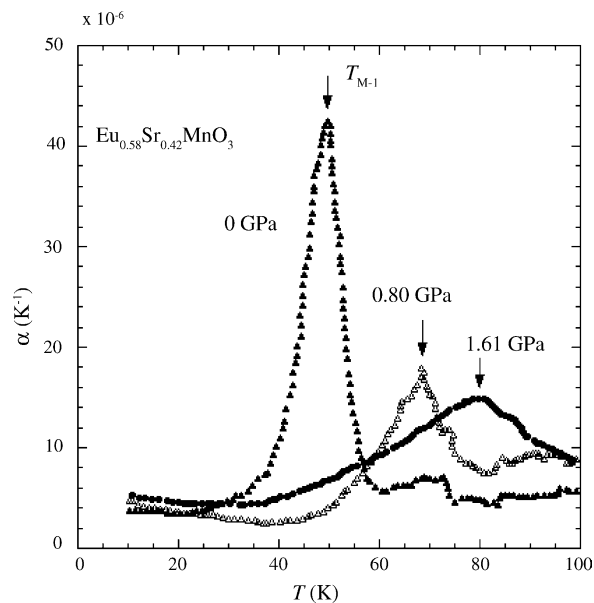


Fig. 3. Thermal expansion coefficients  $\alpha(\text{K}^{-1})$  of FMM phase at high pressure.  $T_{M-I}$  is defined as the temperature with the maximum in  $\alpha(T)$ .

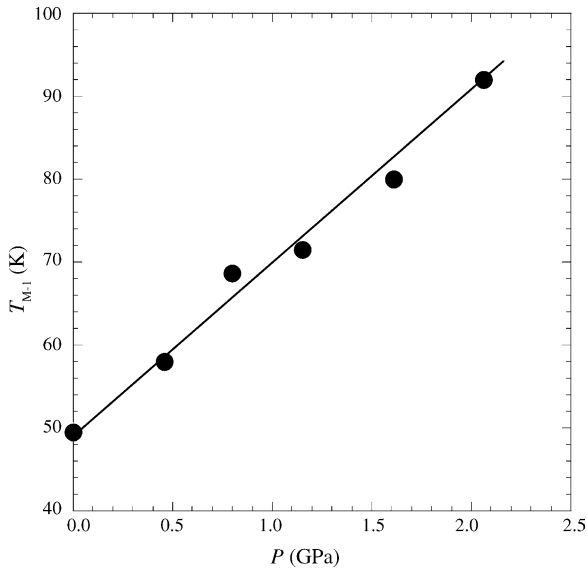


Fig. 4.  $T_{M-I}$  as a function of pressure.

### 3.2. Thermal expansion at high pressure

The thermal expansion  $\Delta L/L$  was measured on heating at high pressure after the sample was cooled down to 4.2 K, magnetic field was applied up to 5 T and then the field decreased to zero. Fig. 2 shows  $\Delta L/L$  of  $\text{Eu}_{0.58}\text{Sr}_{0.42}\text{MnO}_3$  as a function of temperature  $T(K)$  at high pressure up to 2.06 GPa. At ambient pressure, an anomalous behavior was observed near 50 K, which corresponds to FMM-CAFMI phase transition or metal-insulator transition temperatures  $T_{M-I}$ . As pressure increases,  $T_{M-I}$  increases and the anomaly occurs in the wide range of temperature and becomes unclear. In order to calculate the thermal expansion coefficients  $\alpha$ , we differentiate  $\Delta L/L(T)$  curves with respect to  $T$ . The results are shown in Fig. 3 as a function of  $T$  at various pressures. In the  $\alpha(T)$  curve, a peak is found at each pressure. We defined the metal-insulator transition temperature  $T_{M-I}$  as a temperature where  $\alpha(T)$  shows a peak. Fig. 4 shows  $T_{M-I}$  as a function of pressure. It is seen that the half width of peak becomes wide and the peak height decreases as pressure increases.  $T_{M-I}$  is found to increase with increasing pressure approximately in linear fashion against pressure having a coefficient,  $dT_{M-I}/dP = 21 \text{ K/GPa}$ .

### 3.3. Magnetostriction at high pressure

Fig. 5 shows the magnetostriction as a function of magnetic field  $H(T)$  at various pressures. At ambient pressure,  $\Delta L/L(H)$  at 6 K begins to decrease near 1 T, followed by a sudden decrease of about  $0.4 \times 10^{-3}$  and above 2.5 T it shows a small change up to 5 T. On decreasing  $H$ ,  $\Delta L/L$  increases slightly without any discontinuity. The magnetic state after releasing  $H$  is considered to be in FMM. The large change around 2 T is first order phase transition accompanied by a large hysteresis. The electronic state below 1 T

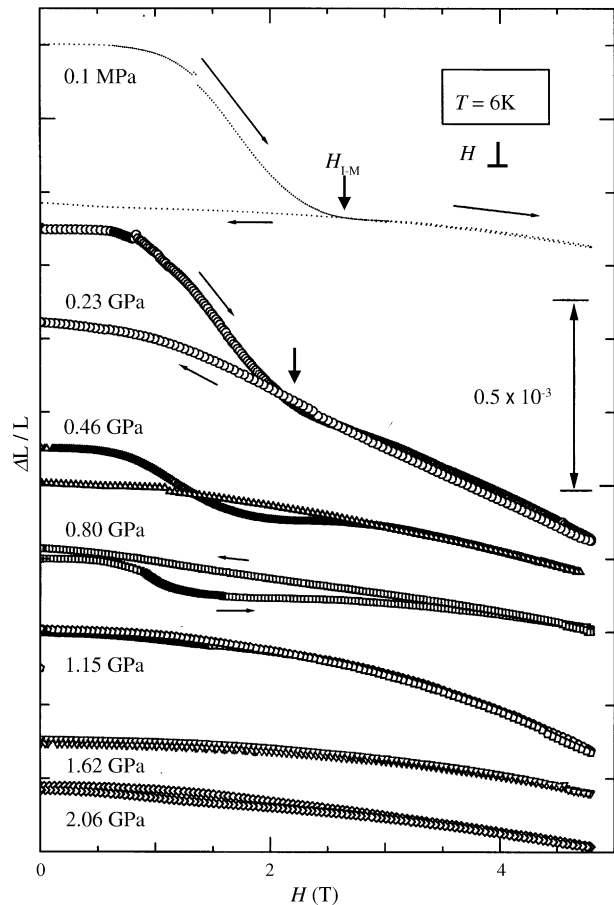


Fig. 5. Magnetostriction perpendicular to  $H$  at various pressures. The arrows show the direction of change in  $H$ .

corresponds to spin glass insulator and antiferromagnetic insulator (AFMI) in the range between 1 and 2.5 T, and then FMM above 2.5 T [2]. By increasing pressure, the jump in  $\Delta L/L$  due to AFMI  $\rightarrow$  FMM phase transition is suppressed and finally disappears at 1.15 GPa. These results are in good agreement with the previous one obtained by measuring the electrical resistance [3]. The magnetic field where the change

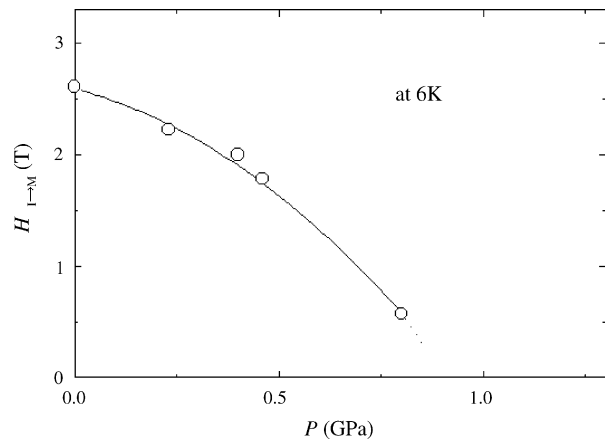


Fig. 6. The pressure dependence of  $H_{I \rightarrow M}$  showing field-induced insulator  $\rightarrow$  metal transition at 6 K.

in  $\Delta L/L$  is 0 is defined as  $H_{I \rightarrow M}$ . Fig. 6 shows  $H_{I \rightarrow M}$  as a function of pressure, in which  $H_{I \rightarrow M}$  becomes zero around 0.9 GPa.

#### 4. Discussion

The spontaneous volume magnetostriction,  $\omega_s(T = 0) = \omega_s(0)$ , which is approximated as  $\omega_s(T = 6 \text{ K})$ , is three times the difference between  $\Delta L/L$  at  $H = 0$  before applying  $H$  and  $\Delta L/L$  at  $H = 0$  after releasing  $H$ . Fig. 7 shows the values of  $\omega_s(0)$  as a function of pressure, along with the previous results for the Néel temperature  $T_N$  and saturation magnetization  $M_s$  [8]. Since  $\omega_s$  is related to  $M_s$  as  $\omega_s = \kappa C M_s^2$ , where  $\kappa$  and  $C$  are the compressibility and magnetoelastic coupling constant [9], the result of the pressure dependence of  $\omega_s$  is qualitatively in agreement with that of  $M_s$ .

Next in order to evaluate the stability of electronic state, we estimate the Grüneisen parameter defined as,  $\Gamma(T_0) = -\partial \ln T_0 / \partial \ln V$ , where  $T_0$  is a characteristic temperature such as Néel temperature, Kondo temperature and so forth. This equation is rewritten as  $\Gamma(T_0) = B_T(1/T_0)(\partial T_0 / \partial P)$ . Using  $B_T = 213 \text{ GPa}$  and the data in Figs. 4, 6 and 7, we obtain the following values for AFMI  $\rightarrow$  FMM transition,

$$\Gamma(T_N) = -117 \quad \text{and} \quad \Gamma(H_{I-M}) = -138. \quad (1)$$

Similarly for the FMM  $\rightarrow$  CAFMI transition, we have

$$\Gamma(T_C) = 74 \quad \text{and} \quad \Gamma(T_{I-M}) = 87. \quad (2)$$

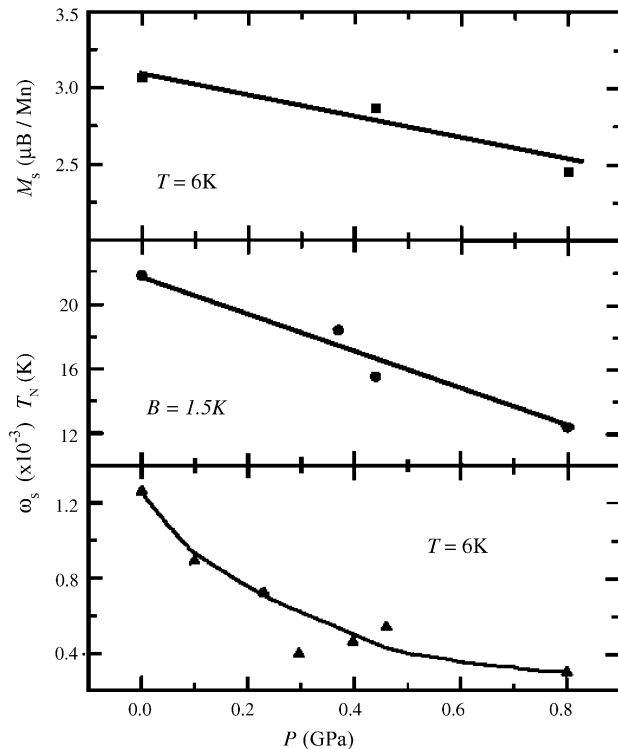


Fig. 7.  $M_s$  at 6 K,  $T_N$  at 1.5 T and  $\omega_s$  at 6 K as a function of pressure.

Here we used the data for the pressure dependence of  $T_C$  [8].

These two values for each characteristic temperature or field are regarded to be nearly the same. It should be surprising that these values are extremely large, which are the same order of magnitude of heavy Fermions [10]. These facts imply that the electronic state of  $\text{Eu}_{0.58}\text{Sr}_{0.42}\text{MnO}_3$  is in marginal state because this sample is considered nearly on the border of metal–insulator and antiferromagnetic–ferromagnetic phase transition, which results in a large Grüneisen parameter.

Finally we suggest the structural change by applying  $H$ . The crystal structure of  $\text{Eu}_{0.58}\text{Sr}_{0.42}\text{MnO}_3$  is orthorhombic at room temperature. The magnetostriction at high pressure is shown in Fig. 5 as a function of  $H$ . The length decreases abruptly near 1 T, which indicates the first order phase transition. This is reminiscent of the first order orthorhombic(O)–rhombohedral(R) phase transition induced by applying  $H$  in  $\text{La}_{1-x}\text{Sr}_x\text{MnO}_3$  near  $x = 0.17$  [11], in which the length decreases discontinuously around 1 T with the magnitude of  $10^{-4}$ . Considering that the crystal structure is the same as that of  $\text{Eu}_{0.58}\text{Sr}_{0.42}\text{MnO}_3$  and the magnitude of discontinuous change in length is the same order, we expect the same transition from O to R to occur by applying  $H$  in  $\text{Eu}_{0.58}\text{Sr}_{0.42}\text{MnO}_3$ .

#### 5. Conclusion

The main results in the present work are summarized as follows:

1. The orthorhombic crystal structure is stable up to 14 GPa at room temperature and the bulk modulus is obtained to be 213 GPa, which is large compared with other oxides.
2. The volume magnetostriction on the metal–insulator transition is about  $1.2 \times 10^{-3}$  at ambient pressure, which decreases by applying pressure and disappears above 0.9 GPa.
3. The structural change induced by applying the magnetic field is suggested but it disappears at high pressure.

#### References

- [1] see for example A.P. Ramirez, J. Phys.: Condens. Matter 9 (1997) 8171.
- [2] A. Sudaresan, A. Maignan, B. Raveau, Phys. Rev. B 55 (1997) 5596.
- [3] I. Kosaka, F. Honda, T. Kagayama, G. Oomi, E.V. Sampathkumaran, A. Sundaresan, Physica B 281 & 282 (2000) 500.
- [4] G. Oomi, T. Kagayama, Physica B 239 (1997) 191.
- [5] T. Kagayama, G. Oomi, J. Magn. Magn. Mater. 140–144 (1995) 1227.
- [6] K. Suenaga, G. Oomi, J. Phys. Soc. Jpn. 60 (1991) 1189.
- [7] T. Kagayama, G. Oomi, J. Mater. Process. Technol. 85 (1999) 229.
- [8] T. Eto, G. Oomi, E.V. Sampathkumaran, A. Sundaresan, M. Kosaka, Y. Uwatoko, J. Magn. Soc. Jpn. 25 (2001) 723.
- [9] G. Oomi, N. Mori, J. Phys. Soc. Jpn. 50 (1981) 2924.
- [10] T. Kagayama, G. Oomi, J. Phys. Soc. Jpn. 65 (1996) 42.
- [11] A. Asamitsu, Y. Morimoto, R. Kumai, Y. Tomioka, Y. Tokura, Phys. Rev. B 54 (1996) 1716.